Hindawi Publishing Corporation
Advances in Materials Science and Engineering
Volume 2010, Article ID 789541, 6 pages
doi:10.1155/2010/789541

Research Article

Synthesis of Nanoporous TiO_2 and Its Potential Applicability for Dye-Sensitized Solar Cell Using Antocyanine Black Rice

Brian Yuliarto,[1] Wilman Septina,[1] Kasyful Fuadi,[1] Fahiem Fanani,[1] Lia Muliani,[2] and Nugraha[1]

[1] *Material Processing Laboratory, Engineering Physics Department, Bandung Institute of Technology, Jl. Ganesha, no.10 Bandung 40132, Indonesia*
[2] *Research Center for Electronics and Telecommunications, Indonesian Institute of Science, Jl. Sangkuriang Kampus LIPI Gd 20 Bandung 40152, Indonesia*

Correspondence should be addressed to Brian Yuliarto, brian@tf.itb.ac.id

Received 21 April 2010; Revised 13 July 2010; Accepted 5 September 2010

Academic Editor: Steven Suib

Nanoporous mesostructure TiO_2 powders were synthesized by sol-gel method, with $TiCl_4$ as a precursor in methanol solution. The Pluronic PE 6200 of block copolymer was used as the pores template. It was found from XRD measurements, both at 400°C and 450°C calcination temperatures, that the sol-gel technique yielded the nanoporous TiO_2 with anatase phase. Based on N_2 adsorption characterization using BET method, the TiO_2 samples have surface area of 108 m^2/g and 88 m^2/g for calcination temperatures of 400°C and of 450°C, respectively. From small-angle neutron scattering (SANS) patterns, TiO_2 samples were observed to have nanoporous structures with pore sizes between 22–24 nm. The TiO_2 also have order degree which depends on the calcination temperature. The potential applicability of the resulting TiO_2 is confirmed for dye-sensitized solar cell (DSSC), composed of nanoporous anatase TiO_2 and natural dye from antocyanine black rice. UV-Vis measurement of dye extracted from the black rice indicated that the antocyanine chelate can propagate into the TiO_2 nanoporous network. The short circuit photocurrent density (Jsc) under 100 $mWcm^{-2}$ reached 1.287 $mAcm^{-2}$ with open circuit photovoltage (Voc) of 550 mV and the fill factor of 33.4%. The results show that the hybrid organic-inorganic structures are very attractive for future low-cost devices.

1. Introduction

The dye-sensitized solar cell (DSSC) is one of the potential candidates for next generation solar cells, because its low-cost material and relatively simple production processes. Different from conventional solar cells whose working principle is based on solid state theory, dye-sensitized solar cell is a photoelectrochemical-based solar cell. Photo absorption is done by dye molecule and charge separation by inorganic semiconductor nanocrystals which have a large band gap, and uses electrolytes for dye regeneration.

One of the commonly used wide gap semiconductor for DSSC applications is titanium dioxide (TiO_2). Titanium dioxide (TiO_2) is a semiconductor material which has wide applications in optical as well as electronics materials. This is because TiO_2 have remarkable physical, chemical, and optical characteristics. It has attracted increased attention for potential applications as gas sensors [1], metal-oxide-semiconductor field effect transistors (MOSFET) gate dielectric [2], anti-microbial coating [3], pigments [3], solar hydrogen generation [4], and photovoltaic cells or well known as dye-sensitized solar cell (DSSC) [5]. In energy and environmental fields, much research has been done on TiO_2 characteristics especially on its applications as a main component of DSSC [3]. For this application, material with large surface area is preferred to increase the contact area. Indeed the nanostructure of TiO_2 becomes an important characteristic as well as the pore nanosize. A certain class of nanoporous material emerged from the requirements called mesoporous material, which has pore diameters between 2–50 nm [4]. This kind of material has attracted much attention because of its wide potential applicability in dye-sensitized solar cells as well as sensor devices [5–10].

Mesoporous TiO_2 has been developed with various methods, most importantly using organic templates to build porous structures. Synthesis of mesoporous TiO_2 was first reported by Antonelli and Ying in 1995 using an ionic alkyl phosphate surfactant as a template with sol-gel method [11], however the resulting material was not pure TiO_2 because the phosphate molecules were strongly bonded on to the TiO_2 structure. One alternative is to use nonionic surfactants, particularly block copolymers, as a substitute to ionic surfactants. Block copolymers have an advantage of being easily removed from inorganic frameworks by calcination or solvent extraction since the block copolymer only involves H-bonding type rather than the electrostatic interactions found using ionic surfactant [12]. Moreover the properties of block copolymers can be continuously tuned by adjusting solvent composition, molecular weight, or polymer architectures of block copolymers [13].

After succeeding in synthesizing mesoporous material using block copolymer templates, publications related to mesoporous TiO_2 has continuously increased, but mostly used titanium alkoxide as Ti source at aqueous solution [14]. Large amounts of water inside the solution can cause hydrolysis and condensation as well as difficulties in controlling the mesostructure because the alkoxide is highly reactive with water. In this research we firstly, in our knowledge, prepared mesoporous TiO_2 using triblock copolymer Pluronic PE 6200 as a template and $TiCl_4$ as a precursor at alcoholic solution. The resulting mesostructure TiO_2 powder is characterized by using X-ray diffraction, SEM, and small-angle neutron scattering (SANS) to confirm the nanostructure of materials. The resulting mesostructure TiO_2 has a nanocrystalline wall, which is necessary to ensure good electron diffusion [15]. A DSSC using nanocrystalline TiO_2 film electrode is then fabricated and a DSSC using visible light sensitisation of a nanocrystalline TiO_2 film is developed.

To investigate TiO_2 application in a DSSC system, the use of natural dye extracted from antocyanine black rice was investigated. Natural antocyanine from black rice extraction would be used as the dye since the antocyanin has good chemical bonding with titanium dioxide [16]. The I-V curve measurement was performed under direct Xenon HID lamp using multimeter, variable resistor, and pyranometer.

2. Experimental Method

The triblock copolymer PEO-PPO-PEO Pluronic PE 6200 (PEO_8-PPO_{30}-PEO_8, M_{av} = 2450 g/mol) was supplied by BASF. The titanium tetrachloride ($TiCl_4$) precursor was purchased from Merck, and methanol was used as a solvent. To obtain TiO_2 paste, polyvinyl alcohol (PVA) was used. The dye was extracted from the black rice. All chemicals were used without further purification.

An initial solution was made by adding 1 gram of Pluronic PE 6200 to 10 gram methanol and stirred for 30 minutes to initiate micelle structure. Then the $TiCl_4$ was slowly added to the solution under stirring for 30 minutes so that the molar ratio of $TiCl_4$: methanol : Pluronic PE6200 was 1 : 21.7 : 0.0408. The ratios used in the synthesis process are as follow; $TiCl_4$: methanol : Pluronic PE6200. $TiCl_4$ reaction with alcoholic solution is exothermic and produces large amount of HCl gas and a collection of chloroalkoxide ($TiCl_2(OCH_3)_2$) [17, 18]. The solutions were then aged for 4 days at 40–45°C in a furnace until dry gel was formed. The TiO_2 dry gels were then calcined at 400°–450°C for 4 hours with a heating rate of 5-6°C/minute to remove the block copolymer and promote crystallization.

The TiO_2 paste was made by mixing TiO_2 powder with 10% polyvinyl alcohol (PVA)/water solution, mixed at 80°C. After that the resulting powder was ground with mortar to obtain the smooth paste for deposition. The paste was deposited onto ITO conductive glass (In:SnO_2) using doctor blade technique with area of 0.855 cm^2, then sintered at 450°C for 30 minutes. The TiO_2 film was then rinsed in dye solution extracted from black rice for about 30 minutes.

The antocyanine dye was derived from Indonesian black rice extraction using organic solvent which is the combination of alcohol, acetic acid, and water with the molar ratio of 25 : 4 : 21. The black rice as much as 13 gram was grinded using mortar then dissolved by solvent on magnetic stirrer. Finally, the solid filtrate was removed with filtration paper and the dye was kept in tight and dark bottle to prevent evaporation and degradation.

The conductive glass with platinum layer as a catalyst was put on the top of the TiO_2-dye electrode. This platinum-conductive glass acted as a counter electrode. The electrolyte for dye regeneration is composed of 0.5 M potassium iodide (KI), 0.05 M Iodine (I_2), and acetonitrile solvent (all obtained from Merck).

3. Results and Discussion

Figure 1 shows Thermo Gravimetric-Differential Thermal Analysis (TG-DTA) results for TiO_2 dry gel after 4 days aging at 45°C. The TG-DTA was performed at the temperature range between 50°–600°C with 10°C/minute of heating rate. From the TGA curve, which shows sample weight loss as the function of temperature, the sample weight decreased by about 75% when heated up to 460°C. The TGA curve also shows three weight-loss regions. The first region of temperatures below 200°C resulted from –OH groups evaporation. The second region between 200°– 325°C was attributed to organic decomposition. The third region from 325°C to 460°C is due to residual block copolymer oxidation and decomposition of chlorine bonded to the Ti-OH. The TGA curve also shows that the block copolymer was completely removed at calcination temperatures above 450°C.

The DTA curve clearly shows two peaks, the endothermic peak at region of 100°C–200°C which is attributed to solvent evaporation, and broad exothermic peak at 325°C–460°C which is attributed to the decomposition of block copolymer and chlorine and phase transformation from amorphous to anatase TiO_2. The phase transformation actually starts from 350°C [19]. As shown in the full TG-DTA curve, the data from TGA curve correlates directly to the DTA record

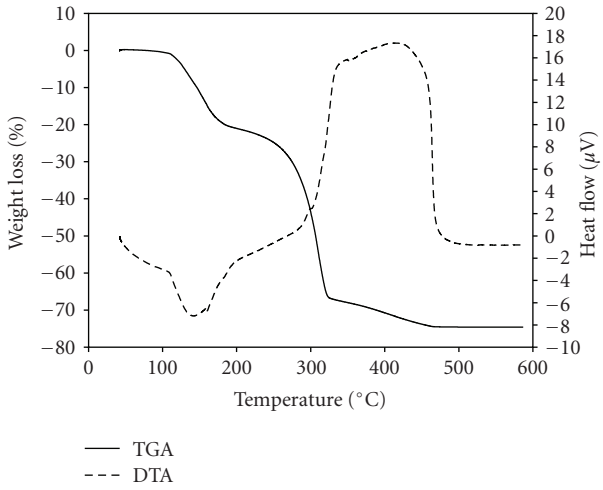

Figure 1: TG-DTA results for TiO_2 dry-gel where the TGA: full line and DTA: dashed line.

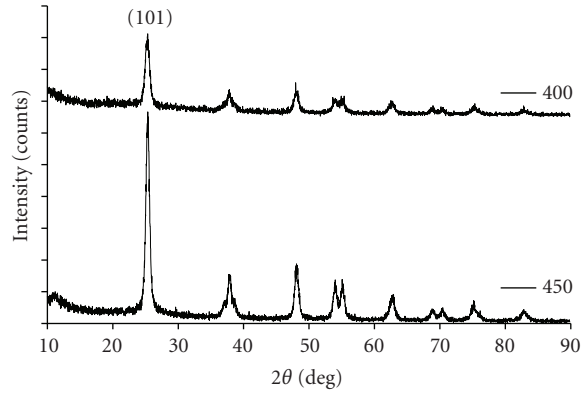

Figure 2: Wide-angle XRD patterns of nanoporous TiO_2.

since the weight-losses are always followed by endothermic or exothermic processes.

The X-Ray Diffractometer (XRD) patterns were obtained using Philips Analytical X-Ray with Cu radiation (λ = 0.154056 nm) and the crystallite sizes were calculated using Scherrer equation at Miller indices (101). Wide-angle XRD patterns shown at Figure 2 indicate both samples have well-crystallized TiO_2 with pure anatase phase according to the JCPDS number 21-1272. As shown at Table 1, higher calcination temperatures resulted in higher crystallite size. More intense and well-resolved peaks observed at higher calcinations temperature indicate the increasing degree of the crystalline. This result correlated with the fact that full crystallization of TiO_2 occurs at 550°C [20]. In accordance with TG-DTA result, TiO_2 sample calcined below 450°C still contain some residual carbon, which can be observed from black colour of the powder sample, which in turn may contribute to amorphous peak nature at XRD patterns.

Small-angle Neutron Scattering (SANS) measurements were carried out to confirm the porous structure of the resulting TiO_2 at Neutron Scattering Laboratory, BATAN Indonesia using SMARTer. The neutron wavelength of SANS

Table 1: Properties of Nanoporous TiO_2.

Sample	Calcinations Temperature	Particle size[a]	Surface Area (m^2/g)
Ti-a	400°C	11 nm	108
Ti-b	450°C	14 nm	88

[a]Calculated from Scherrer equation at Miller indices (101).

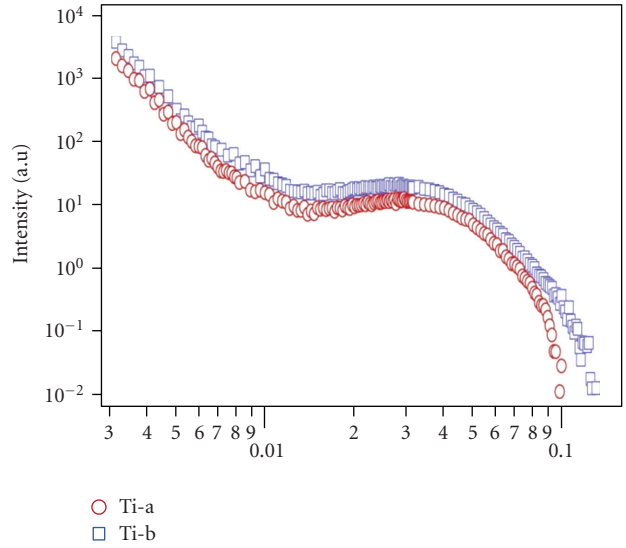

Figure 3: Small-angle Neutron (SANS) patterns of nanoporous TiO_2.

was λ = 0.566 nm. Sample to detector distances were varied at 2, 8, and 18 meter to obtain the vector of transfer momentum (q) range about 0.02–1.5 nm^{-1}. The SANS patterns as shown in Figure 3 confirm that the correlation peak formed at both samples indicated that mesoporous structures were preserved. The peak formed at low angle can be attributed to the distance between the center of pores [20]. According to the calculations, the average pore distances ($d = 2\pi/q_{peak}$) are about 22 nm (Ti-a) and 24 nm (Ti-b) which is typical of the pore to pore distance of mesoporous materials. Average pore distance was increased with increasing calcination temperatures because of structure contraction observed from the heat treatment. SANS patterns also show that the peak intensity of lower calcination temperature sample (Ti-a) was slightly larger. This indicating that sample with lower calcinations temperature has higher pore ordering than sample with higher calcinations temperature (Ti-b).

Scanning Electron Microscope (SEM) images were obtained from JEOL operated at 20 kV. The morphology of the samples was observed with SEM images as shown at Figure 4. The structure morphology contains large amount of close packed particles which is typical of porous material. The mesoporosity of samples was partially due to both intrastructure porosity and interstructure porosity of the materials.

Nitrogen adsorption measurements were carried out on a NOVA 1000 High Speed Gas Sorption Analyzer to determine Brunau-Emmett-Teller (BET) surface area. Before

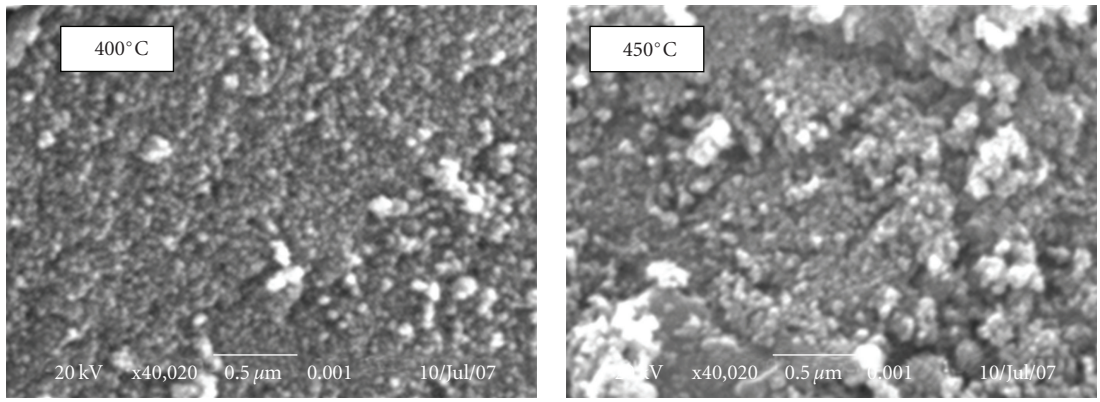

Figure 4: SEM Images of nanoporous TiO_2 calcined at 400°C and 450°C.

these measurements, the samples were degassed at 200°C for 2 hours in vacuum conditions to eliminate water and oil. According to N_2 adsorption measurements, the BET surface area are 108 m^2/g and 88 m^2/g for Ti-a sample and Ti-b sample, respectively (Table 1). Higher calcination temperatures produced a lower surface area since the crystallization of TiO_2 is usually followed by some collapse and destruction of the mesostructure [21]. These surface areas are larger than commercial Degussa P-25 which is mainly used as a nano TiO_2 reference which has BET surface area at about 50 m^2/g [22].

The DSSC performance of the Ti-a sample was investigated using illumination from a solar simulator. Photocurrent-photovoltage characteristic of the black rice adsorbed on a nanocrystalline TiO_2 electrode was measured with a sandwich type cell. The working electrode with the black rice dye adsorbed on a nanocrystalline TiO_2 film was gently squeezed together with a platinum-coated ITO glass electrode and irradiated from the substrate side of working electrode. The I-V curve was characterized using a 10 kΩ potentiometer and digital multimeter (Fluke 77 III and Advantest) to get maximum power output (see Figure 5). Irradiation of 100 mW/cm^2 by a 35 W Xenon HID lamp was measured using Precision Spectral Pyranometer (Eppley Radiometer) to get the intensity. The fill factor (FF) and efficiency (η) are calculated as [1]

$$\mathrm{FF} = \frac{(I_{\max} \times V_{\max})}{(I_{sc} \times V_{oc})}, \tag{1}$$

$$\eta = \frac{(I_{sc} \times V_{oc} \times \mathrm{FF})}{P_{in}}. \tag{2}$$

Figure 6 shows the photocurrent-photovoltage characteristics of a sandwich solar cell based on the black rice dye adsorbed on a nanoporous TiO_2 film electrode irradiated with a light intensity of 100 mW/cm^2 as a light source. The I_{sc}, V_{oc}, I_{max}, V_{max}, and the point of P_{max} also are indicated in Figure 6. The I_{max} and V_{max}, which indicate the photocurrent and photovoltage at P_{max}, are estimated to be 0.69 $mAcm^{-2}$ and 343 mV. The J_{sc} and V_{oc} values of solar cell were estimated to be 1.287 $mAcm^{-2}$ and 550 mV. The η value

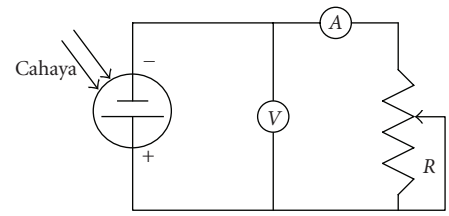

Figure 5: The circuit for the measurement of photocurrent-photovoltage characterization of DSSC using black rice adsorbed on a nanocrystalline TiO_2 film electrode with 35 W HID lamp.

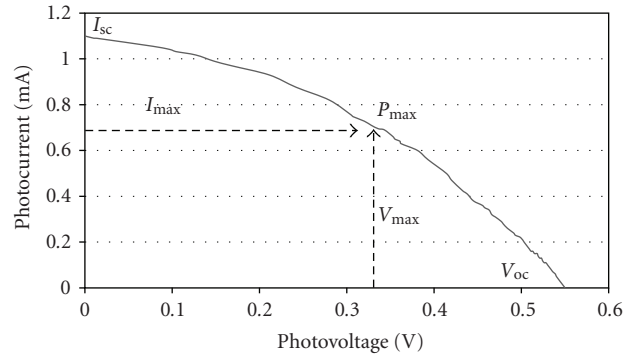

Figure 6: Photocurrent-photovoltage characterization of dye-sensitized solar cell using black rice dye immobilized on TiO_2 film with 35 W Xenon HID lamp as a light source.

was estimated to be 0.236% and the P_{max} was 236.7 μWcm^{-2}. The FF value was estimated to be 33.4% using (1). The low efficiency of DSSC could be caused by the black rice dyes extraction which could be improved by better extraction process such as purification and enrichment.

To investigate the absorption process of sunlight into the black rice dye, the UV-VIS measurement is performed between 200–700 nm of the wavelength. The Figure 7 shows the UV-Vis absorbance spectrum of black rice dye extract which is characterized by three peaks located at 242, 282, and 530 nm, with absorbance 0.72, 0.80, and 0.62, respectively (in arbitrary unit). Those peaks indicate the higher possibility

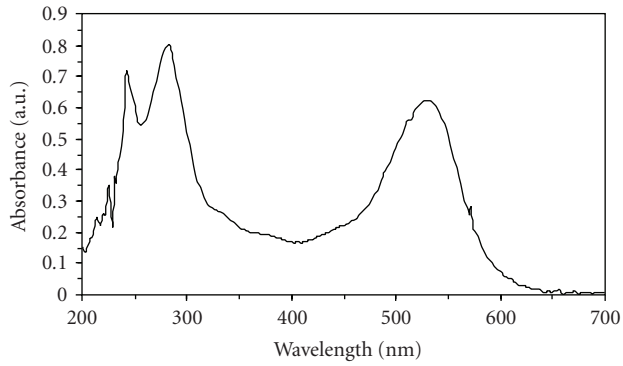

Figure 7: Absorbance spectra of black rice dyes extract.

to absorb sunlight, especially at 530 nm. Because of the peak of sunlight spectra at 550 nm [1], the dyes can receive maximum sunlight absorption. When the antocyanine dyes from black rice chemically bonded with TiO_2, it can be chemical adsorption or chelation as described before; the LUMO-HOMO of dyes will be affected so that the bandgap energy will change. Finally, the changing of bandgap energy will shift the peak of absorbance spectra and broaden the peak. Some reports state that the shifting goes to the lower energy or red shifting [5, 9]. As a result, the black rice dyes absorbance will approach the sunlight maxima spectra, which yield higher possibility of light harvesting.

4. Conclusions

Nanoporous TiO_2 with mesostructure anatase wall have been successfully prepared using a combination of sol-gel method and block copolymer as a template. $TiCl_4$ was used as a Ti precursor and Pluronic PE6200 acted well as mesoporous template although only short-range pore ordering is observed. Calcination temperature was observed to be an important parameter for mesostructure formation as well as crystallization process. The biophotovoltaic conversion device based on DSSC using black rice dye adsorbed nanoporous anatase TiO_2 film electrode was prepared and the DSSC using visible light sensitisation of a nanocrystalline TiO_2 film was developed. The I-V curve of the solar cell using black rice adsorbed on a nanocrystalline TiO_2 electrode is characterized under light intensity of 100 $mWcm^{-2}$. It is estimated that η value was 0.236% and the FF value was 33.4%.

Acknowledgments

This work has been supported by a grant from HIBAH STRATEGIS NASIONAL DIKTI of the Ministry of National Educations. Authors would like to thanks BASF Indonesia for providing block copolymer PE6200 and Dr. Edy Giri from BATAN-Indonesia for his assistance in SANS characterization.

References

[1] K. Hashimoto, H. Irie, and A. Fujishima, "TiO_2 photocatalysis: a historical overview and future prospects," *Japanese Journal of Applied Physics, Part 1*, vol. 44, no. 12, pp. 8269–8285, 2005.

[2] B. Yuliarto, I. Honma, Y. Katsumura, and H. Zhou, "Preparation of room temperature NO_2 gas sensors based on W- and V-modified mesoporous MCM-41 thin films employing surface photovoltage technique," *Sensors and Actuators, B*, vol. 114, no. 1, pp. 109–119, 2006.

[3] M. Grätzel, "Dye-sensitized solar cells," *Journal of Photochemistry and Photobiology C*, vol. 4, no. 2, pp. 145–153, 2003.

[4] C. T. Kresge, M. E. Leonowicz, W. J. Roth, J. C. Vartuli, and J. S. Beck, "Ordered mesoporous molecular sieves synthesized by a liquid-crystal template mechanism," *Nature*, vol. 359, no. 6397, pp. 710–712, 1992.

[5] H. Abdullah, N. P. Ariyanto, S. Shaari, B. Yuliarto, and S. Junaidi, "Study of porous nanoflake ZnO for dye-sensitized solar cell application," *American Journal of Engineering and Applied Sciences*, vol. 2, no. 1, pp. 236–140, 2009.

[6] N. P. Ariyanto, H. Abdullah, S. Shaari, S. Junaidi, and B. Yuliarto, "Preparation and characterisation of porous nanosheets zinc oxide films: based on chemical bath deposition," *World Applied Sciences Journal*, vol. 6, no. 6, pp. 764–768, 2009.

[7] B. Yuliarto, Y. Kumai, I. Honma, S. Inagaki, and H. Zhou, "Benzene sensors based on surface photo voltage of mesoporous organo-silica hybrid thin films," *Studies in Surface Science and Catalysis*, vol. 165, pp. 893–896, 2007.

[8] B. Yuliarto, Y. Kumai, S. Inagaki, and H. Zhou, "Enhanced benzene selectivity of mesoporous silica SPV sensors by incorporating phenylene groups in the silica framework," *Sensors and Actuators, B*, vol. 138, no. 2, pp. 417–421, 2009.

[9] B. Yuliarto, H. Zhou, T. Yamada, I. Honma, Y. Katsumura, and M. Ichihara, "Effect of tin addition on mesoporous silica thin film and its application for surface photovoltage NO_2 gas sensor," *Analytical Chemistry*, vol. 76, no. 22, pp. 6719–6726, 2004.

[10] B. Yuliarto, H. Zhou, T. Yamada, I. Honma, and K. Asai, "Synthesis of a surface photovoltage sensor using self-ordered tin-modified MCM-41 films: enhanced NO_2 gas sensing," *ChemPhysChem*, vol. 5, no. 2, pp. 261–265, 2004.

[11] D. M. Antonelli and J. Y. Ying, "Synthesis of hexagonally packed mesoporous TiO_2 by a modified sol-gel method," *Angewandte Chemie*, vol. 34, no. 18, pp. 2014–2017, 1995.

[12] G. J. D. A. A. Soler-Illia, E. L. Crepaldi, D. Grosso, and C. Sanchez, "Block copolymer-templated mesoporous oxides," *Current Opinion in Colloid and Interface Science*, vol. 8, no. 1, pp. 109–126, 2003.

[13] F. S. Bates and G. H. Fredrickson, "Block copolymers-designer soft materials," *Physics Today*, vol. 52, no. 2, pp. 32–38, 1999.

[14] P. Yang, D. Zhao, D. I. Margolese, B. F. Chmelka, and G. D. Stucky, "Block copolymer templating syntheses of mesoporous metal oxides with large ordering lengths and semicrystalline framework," *Chemistry of Materials*, vol. 11, no. 10, pp. 2813–2826, 1999.

[15] M. C. Fuertes and G. J. A. A. Soler-Illia, "Processing of macroporous titania thin films: from multiscale functional porosity to nanocrystalline macroporous TiO_2," *Chemistry of Materials*, vol. 18, no. 8, pp. 2109–2117, 2006.

[16] S. Hao, J. Wu, Y. Huang, and J. Lin, "Natural dyes as photosensitizers for dye-sensitized solar cell," *Solar Energy*, vol. 80, no. 2, pp. 209–216, 2006.

[17] G. J. D. A. A. Soler-Illia, C. Sanchez, B. Lebeau, and J. Patarin, "Chemical strategies to design textured materials: from microporous and mesoporous oxides to nanonetworks and hierarchical structures," *Chemical Reviews*, vol. 102, no. 11, pp. 4093–4138, 2002.

[18] H. Luo, C. Wang, and Y. Yan, "Synthesis of mesostructured titania with controlled crystalline framework," *Chemistry of Materials*, vol. 15, no. 20, pp. 3841–3846, 2003.

[19] E. L. Crepaldi, G. J. D. A. A. Soler-Illia, D. Grosso, F. Cagnol, F. Ribot, and C. Sanchez, "Controlled formation of highly organized mesoporous titania thin films: from mesostructured hybrids to mesoporous nanoanatase TiO_2," *Journal of the American Chemical Society*, vol. 125, no. 32, pp. 9770–9786, 2003.

[20] E. Lancelle-Beltran, P. Prené, C. Boscher et al., "Nanostructured hybrid solar cells based on self-assembled mesoporous titania thin films," *Chemistry of Materials*, vol. 18, no. 26, pp. 6152–6156, 2006.

[21] H.-S. Yun, K. Miyazawa, I. Honma, H. Zhou, and M. Kuwabara, "Synthesis of semicrystallized mesoporous TiO_2 thin films using triblock copolymer templates," *Materials Science and Engineering C*, vol. 23, no. 4, pp. 487–494, 2003.

[22] L. Saadoun, J. A. Ayllón, J. Jiménez-Becerril, J. Peral, X. Domènech, and R. Rodríguez-Clemente, "1,2-Diolates of titanium as suitable precursors for the preparation of photoactive high surface titania," *Applied Catalysis B*, vol. 21, no. 4, pp. 269–277, 1999.